Redox Biology 11 (2017) 688–700

Contents lists available at ScienceDirect

Redox Biology

journal homepage: www.elsevier.com/locate/redox

Research Paper

Thioredoxin (Trxo1) interacts with proliferating cell nuclear antigen (PCNA) and its overexpression affects the growth of tobacco cell culture

Aingeru Calderón[a,1], Ana Ortiz-Espín[a,1], Raquel Iglesias-Fernández[b], Pilar Carbonero[b], Federico Vicente Pallardó[c], Francisca Sevilla[a], Ana Jiménez[a,*]

[a] Department of Stress Biology and Plant Pathology, CEBAS-CSIC, Campus Universitario de Espinardo, E-30100 Murcia, Spain
[b] Centre for Plant Biotechnology and Genomics (CBGP; UPM-INIA), Campus de Montegancedo, Universidad Politécnica de Madrid, Pozuelo de Alarcón, E-28223 Madrid, Spain
[c] Department of Physiology, Faculty of Medicine, University of Valencia, Av. Blasco Ibañez 15, E-46010 Valencia, Spain

ARTICLE INFO

Keywords:
Glutathione
Nucleus
Proliferating cell nuclear antigen (PCNA)
Cell cycle
Overexpression
Thioredoxin *o*1
Tobacco BY-2 cells

ABSTRACT

Thioredoxins (Trxs), key components of cellular redox regulation, act by controlling the redox status of many target proteins, and have been shown to play an essential role in cell survival and growth. The presence of a Trx system in the nucleus has received little attention in plants, and the nuclear targets of plant Trxs have not been conclusively identified. Thus, very little is known about the function of Trxs in this cellular compartment. Previously, we studied the intracellular localization of PsTrxo1 and confirmed its presence in mitochondria and, interestingly, in the nucleus under standard growth conditions. In investigating the nuclear function of PsTrxo1 we identified proliferating cellular nuclear antigen (PCNA) as a PsTrxo1 target by means of affinity chromatography techniques using purified nuclei from pea leaves. Such protein–protein interaction was corroborated by dot-blot and bimolecular fluorescence complementation (BiFC) assays, which showed that both proteins interact in the nucleus. Moreover, PsTrxo1 showed disulfide reductase activity on previously oxidized recombinant PCNA protein. In parallel, we studied the effects of PsTrxo1 overexpression on Tobacco Bright Yellow-2 (TBY-2) cell cultures. Microscopy and flow-cytometry analysis showed that PsTrxo1 overexpression increases the rate of cell proliferation in the transformed lines, with a higher percentage of the S phase of the cell cycle at the beginning of the cell culture (days 1 and 3) and at the G2/M phase after longer times of culture (day 9), coinciding with an upregulation of PCNA protein. Furthermore, in PsTrxo1 overexpressed cells there is a decrease in the total cellular glutathione content but maintained nuclear GSH accumulation, especially at the end of the culture, which is accompanied by a higher mitotic index, unlike non-overexpressing cells. These results suggest that Trxo1 is involved in the cell cycle progression of TBY-2 cultures, possibly through its link with cellular PCNA and glutathione.

1. Introduction

In plants, abiotic and biotic stresses usually interfere with the redox state of the cells, leading to the generation of excess reactive oxygen and nitrogen species (ROS/RNS) that affect plant growth and development under normal and stress conditions. In addition, ROS and RNS are known to act as signaling molecules in the maintenance of physiological functions and in the response to changing environments [1–3]. In green tissues, although the main sources of ROS are chloroplasts and peroxisomes, mitochondria account for the total production, generating ROS as a product of respiration [4,5], while several reports point to the nuclear compartment as being particularly sensitive to the deleterious effects of oxidation [6]. Furthermore, recent evidence shows that ROS and, particularly H_2O_2, generation occurs as a consequence of DNA damage, suggesting that the nuclear generation of oxidants may also function in cell signaling. In plant cells, experiments

Abbreviations: AMS, 4-acetamido-4-maleimidylstilbene-2,2-disulfonic acid; BiFC, bimolecular fluorescence complementation; BSA, bovine serum albumin; DTT, 1,4-dithiothreitol; DAPI, 4,6-diamidine-2-phenylindol; DEM, diethyl maleate; GFP, green fluorescent protein; mCBM, monochlorobimane; NTR, NADPH thioredoxin reductase; OD, optical density; Oex, overexpressing; PCNA, proliferating cell nuclear antigen; Prx, peroxiredoxin; RNA, reactive nitrogen species; ROS, reactive oxygen species; RT-qPCR, Reverse transcription quantitative polymerase chain reaction; TBS, Tris-buffered saline; TFs, transcription factors; Trx, thioredoxin; TBY-2, tobacco bright yellow-2; YFP, yellow fluorescent protein

* Corresponding author.
E-mail addresses: acalderon@cebas.csic.es (A. Calderón), amortiz@cebas.csic.es (A. Ortiz-Espín), raquel.iglesias@upm.es (R. Iglesias-Fernández), p.carbonero@upm.es (P. Carbonero), Federico.V.Pallardo@uv.es (F.V. Pallardó), fsevilla@cebas.csic.es (F. Sevilla), ajimenez@cebas.csic.es (A. Jiménez).
[1] These authors contributed equally to the work.

http://dx.doi.org/10.1016/j.redox.2017.01.018
Received 25 November 2016; Received in revised form 19 January 2017; Accepted 26 January 2017
Available online 31 January 2017

performed in tobacco (*Nicotiana tabacum* L.) Bright-Yellow-2 (TBY-2) nuclei also suggest that this compartment may not only be invaded by ROS diffusing from neighboring compartments but is also an active source of ROS, in particular of H_2O_2 [7], which has been implicated in the regulation of plant development, the cell cycle and the induction of plant defense responses during stress adaptation, as well as in plant cell death [8,9].

These reactive molecules may perturb cellular homeostasis, and some protein cysteine residues are highly sensitive to oxidation due to the reactivity of their thiol groups, which may interrupt cellular homeostasis [10,11]. The redox state of plant thiols and the regulation of cysteinyl residues in proteins are emerging as key players in the response of plants to different stresses, as well as in plant development, functioning in the redox sensing and signal transduction pathways. Thiol reduction is mainly controlled by the thioredoxin (Trx)/peroxiredoxin (Prx) and glutathione (GSH) systems, which modulate redox signaling during development and stress adaptation [12–15]. Thioredoxins are small proteins containing two cysteines in the redox active center and they are involved in the reduction of disulfide bonds of other proteins through a dithiol-disulfide exchange mechanism. In plants there are at least ten families of Trxs, with more than 40 members present in almost all cellular compartments [16]. The diversity of isoforms seems to support the idea that plants have an additional antioxidant system compared to mammals, where only two types of Trxs have been described, Trx1 and Trx2, in the cytosol/nucleus and mitochondria, respectively [17].

The presence of Trx in plant mitochondria was demonstrated in Arabidopsis [18], where it was classified as Trx*o* type (AtTrx*o*1). More recently, we described how pea Trx*o*1 is located in both the mitochondria and nucleus under physiological non-stressed conditions [19], while several cytosolic Trx*h* isoforms accumulate in the nucleus of developing wheat aleurone and scutellum cells during oxidative stress [20], subsequent studies describing a functional thioredoxin system in the plant nucleus [21]. However, in general, little has been published on the presence of Trxs in the nucleus in plants. In mitochondria, and in cytosol, these oxidoreductases are reduced with electrons from NADPH by compartment-specific NADPH/TRX reductases (NTRs), whereas the chloroplast Trxs are reduced by the electrons provided by photosynthetic electron transport [22]. In animal systems, on the other hand, cytosolic/nuclear Trx1 has been well characterized. Stress-induced Trx1 accumulates in the nucleus to get the required redox state of the transcription factors (TFs) to bind the promoter region of DNA, acting as a master regulator of transcription. For example, Trx1 induces transcriptional activity of NF-kB increasing its ability to bind to DNA [23]. It is also required to resist apoptosis, probably by regulating the apoptotic gene p53 [24]. In plants, some redox-regulated TFs under retrograde regulation have been described in response to stress. Trx*h*5 has been reported as involved in the reported redox regulation of NPR1 allowing its translocation to the nucleus, to activate redox-sensitive TGA [25]. In sugarcane, Trx*h*1 has been identified as an interacting partner of the redox-regulated TF SsNAC23, which is a member of the plant-specific NAC TF family, with roles in development and the response to cold stress [26].

Furthermore, previous evidence supports the view that cellular redox homeostasis is a crucial regulator of cell fate in mammals and plants, and that an intrinsic redox cycle consisting of reductive and oxidative phases can exert a major influence over cell cycle progression [27]. Trx has been shown to be necessary for cell-cycle progression in *E. coli* [28] and *Xenopus* [29]: more specifically, its lack in yeast induces cell-cycle arrest at G1 to S phase [30], acting as the physiological electron donor for ribonucleotide reductase (RNR) during DNA precursor synthesis [31,32]. In the human system, Trx is reported to enhance cell growth [33], whereas in plants, the Trx system and glutathione are involved in the control of the postembryonic development of the shoot apical meristems [34]. Moreover, accumulated evidence shows that in both mammalian and plant cells, glutathione (GSH) concentrates in the nucleus in the early phases of cell growth, where it fulfills a number of important functions [35,36].

Recently we reported that the overexpression of PsTrx*o*1 caused significant differences in the response of a TBY-2 cell culture to high concentrations of H_2O_2, consisting of a higher and maintained viability in over-expressing cells, while non-overexpressing lines suffered a severe decrease in viability and marked oxidative stress, with generalized and rapid cell death. All these data pointed to PsTrx*o*1 as a pivotal factor responsible for the delay in the programmed cell death provoked by the H_2O_2 treatment [37]. However, to the best of our knowledge, there is no information on the functional involvement of Trx*o*1 in the nucleus. Previous biochemical and proteomic approaches have been developed to identify target proteins of different thioredoxins, and among the high number of proteins detected, some were nuclear proteins. Only a few of these candidate proteins have been experimentally validated [38]. Thus, to increase our knowledge of the potential nuclear functions of Trx*o*1, we first followed a proteomic approach to identify possible target proteins, using a purified nuclear preparation obtained from pea (*Pisum sativum* L.) leaves. As a result, proliferating cell nuclear antigen (PCNA) was identified as a putative PsTrx*o*1 target. This was confirmed by dot blot analysis and bimolecular fluorescence complementation (BiFC) assays, which revealed that PsTrx*o*1 and PCNA interact in the nucleus. PCNA is a key component of the DNA replication machinery present in the nuclei of all dividing cells, where it plays a central role connecting different DNA metabolic pathways [39,40]. Therefore, to further understand the relationship between both Trx*o*1 and PCNA proteins, an *in vitro* oxido-reductase enzymatic assay was carried out. Furthermore, PsTrx*o*1 overexpressing TBY-2 cell cultures were used to study the function of thioredoxin in living cells, analyzing the effects on cell growth as well as on the PCNA and glutathione content and its cellular localization by flow cytometry. Taken as a whole, the flow cytometry results suggest that Trx*o*1 is involved in cell cycle progression, possibly providing a reductive nuclear environment and interacting with PCNA. All these data may represent a key aspect linking the influence of Trx*o*1 on GSH and PCNA to the observed changes in TBY-2 cell cycle progression.

2. Material and methods

2.1. Plant material, culture growth conditions and growth measurement

Stable PsTrx*o*1 over-expression lines of *Nicotiana tabacum* 'Bright Yellow-2′ (TBY-2) suspension cells were generated as reported [37], and two of these lines and a control GFP line were used. The suspension of tobacco cells was routinely propagated and cultured at 26 °C and a stationary culture was diluted 4:100 (v/v) in new medium according to [41]. The growth of the cell culture was measured by optical density at 600 nm [42].

2.2. Protein extracts

50 mL of TBY-2 culture at different days of growth were centrifuged at 3000*g* for 5 min at 4ºC and resuspended in extraction buffer 100 mM Tris-HCl pH 7.5, 20 mM DTT, 10 mM EDTA, 0.2% Triton X-100, 1 mM PMSF. After 30 1-s-long pulses of sonication on ice, the homogenate was centrifuged at 15,000*g* for 15 min at 4ºC and the supernatant was incubated with 1% streptomycin sulfate for 20 min at room temperature to precipitate the DNA after centrifugation at 15,000*g* at room temperature. The supernatant was kept at 80 °C until use for western blot analysis. Total proteins were determined using the Bradford assay [43].

2.3. Antibodies and recombinant proteins

Monoclonal antibody against PCNA (clone PC10, mouse) was

purchased from Sigma-Aldrich Química (Spain), anti-glutathione antibody [D8] was from Abcam (UK) and the anti-PsTrx*o*1 polyclonal antibody was generated against the C-terminal sequence ARLNHITEKLFKKD as previously reported [19]. Goat anti-rabbit and goat anti-mouse antibodies conjugated to alkaline phosphatase (Boehringer Mannheim, Germany) were used as secondary antibodies. Recombinant human PCNA-138H (HsPCNA) was supplied by Creative biomart® (USA). Recombinant PsPCNA was expressed and purified as follows. *Pisum sativum* RNA from leaves was extracted using an RNeasy Mini Kit (Qiagen, Germany) following the manufacturer's instructions. 2 μg of total RNA was reverse transcribed with the High Capacity cDNA Reverse Transcription Kit (Applied Biosystems, Spain). The coding sequences of PsPCNA were amplified using the Platinum Pfx DNA Polymerase Kit (Invitrogen, Germany) (45 cycles of 30 s at 94 °C, 30 s at 65ºC, and 60 s at 72 °C) with the following primers:

attB1- PsPCNA, AAAAAAGCAGGCTTCATGTTGGAACTCCGTCTCGTT

attB2-PsPCNA, CAAGAAAGCTGGGTCCTATCAGACTAAGCTTGTGGTTTGG

The recognition sequences for BP Recombinase II (Invitrogen, Germany) are underlined. The PCR product was purified and cloned, by site-specific recombination, performed with Gateway BP Clonase II enzyme mix (Invitrogen, Germany), following the manufacturer's instructions, into the entry vector pDONR221 (Invitrogen, Germany) and sequenced. Then, the coding sequence of PsPCNA was subcloned with the restriction enzymes *Xba*I and *Bam*HI (Invitrogen, Germany) into the expression vector pET13 using T4 Ligase (Invitrogen, Germany). This construction was used to transform *Escherichia coli* strain BL21(DE3) grown in 1 l of Luria-Bertani medium containing ampicillin (50 μg/mL) to reach an $OD_{600\ nm}$ of 0.5 at 37ºC. PsPCNA expression was induced for 6 h at 37ºC by adding IPTG (isopropyl b-thiogalactoside) to a 0.4 mM final concentration. Cells were centrifuged at 7000*g* for 10 min, and bacterial pellets were resuspended in a 50 mL of 25 mM lysis buffer Tris-HCl pH 7.5 containing 0.2% PMSF, 0.1% Triton X-100 and 125 mM NaCl. After three freezing cycles, the insoluble material was removed by centrifugation for 15 min at 15,000*g* on ice. The supernatant was then fractionated with ammonium sulfate (40–85% p/v saturation) and the pelleted proteins were dissolved in the above buffer. Then the sample was fractionated by Sephacryl S-200 using a FPLC system (GE Healthcare, UK). The same buffer and fractions containing the protein were pooled and concentrated by dialysis using Amicon Ultra-0.5 mL Centrifugal Filters (Merck Millipore).

The recombinant protein AtNTRA2 was kindly provided by Dr. JJ Lázaro (EEZ-CSIC, Granada, Spain).

2.4. Nuclei isolation

For the isolation of semipure nuclei from pea leaves (80 g), the Plant Nuclei Isolation Extraction Kit (CelLytic PN; Sigma-Aldrich Química (Spain)) was used following the manufacturer's instructions.

2.5. Identification of nuclear Trx*o*1 target proteins

Nuclear proteins were isolated from pea leaves as described above. For the identification of nuclear target proteins we followed essentially the method previously described in [19]. Briefly, in each experiment, around 2 mg of recombinant protein PsTrx*o*1C37S was incubated with 20 mM 1,4-dithiothreitol (DTT, Sigma-Aldrich Química, Spain) for 1 h at 4 °C and then filtered through Sephadex G25 to eliminate DTT, and eluted in 20 mM Tris-HCl buffer pH 7.9 containing 50 mM NaCl, 5% glycerol (v/v) and 1 mM PMSF. The reduced sample was bound to 400 μL of coaffinity resin prepared in the same buffer (TALON Clontech, Takara Bio USA) and maintained by gently shaking at 4 °C for 16 h. Afterwards the sample was centrifuged at 200*g* and washed twice with the same buffer and finally resuspended in the extract containing 1 mg of nuclear proteins. The mixture was maintained by gently shaking at 4 °C for 16 h. Washing and elution of intact Trx target disulfide complexes with imidazole were performed as described by the manufacturer. Two-dimensional non-reducing and reducing SDS-PAGE was performed for the optimal overall resolution of Trx and target proteins.

2.6. Proteomic characterization

The proteins of interest were excised from gels and subjected to automated reduction, alkylation, and digestion with sequencing-grade bovine pancreas trypsin (Roche) in the Proteomic Service of the CNB-CSIC (Centro Nacional de Biotecnología, Madrid, Spain), using a Proteineer DP (Bruker-Daltonics) following the manufacturer's instructions. The tryptic peptide mixtures were analyzed with a MALDI Ultraflex (Bruker-Daltonics) LIFT-MS/MS [44]. The automatic analysis of the data was carried out with the software flexAnalysis (Bruker-Daltonics™). Data from MALDI-MS and MS/MS were combined using the BioTools program (Bruker-Daltonics) to search in the non-redundant data bases (NCBInr and SwissProt) using the Mascot (Matrix Science, UK) software. All data were manually revised using the BLAST protein program (www.expasy.org).

2.7. Protein dot blot

4 μg of PsPCNA and PsTrx*o*1 recombinant proteins were spotted onto four nitrocellulose membranes (Hybond, Amersham Pharmacia, UK), which were blocked by incubation in TBST buffer (25 mM Tris-HCl pH 7.5 containing 1% (w/v) bovine serum albumin (BSA, Sigma-Aldrich Química, Spain) and 0.1% (v/v) Tween-20) for one hour at room temperature. Then, the membranes were overlaid with 0.1 mg/mL of recombinant proteins PsPCNA (A and C) or PsTrx*o*1 (B and D) in TBST and incubated for 2 h at room temperature. BSA protein was also spotted as a control. Membranes A and D was revealed with monoclonal anti-PCNA antibody PC10 (1:1500, Sigma-Aldrich Química (Spain) and membranes B and C with polyclonal anti-PsTrx*o*1 (Martí et al., 2009), diluted in Tris-buffered saline (TBS) containing 1% (w/v) BSA and 0.1% (v/v) Tween-20. After extensive washing with TBS containing Tween 20, the membranes were incubated with the appropriate IgG conjugated to peroxidase. Immunodetection was performed using NBT/BCIP (Roche, Germany) according to the manufacturer's instructions.

2.8. Western blot analysis

For western blot analysis, equal amount of total proteins from TBY-2 cells (30 μg) were resolved using non-reducing 15% SDS–PAGE as described by [45] and transferred onto a nitrocellulose membrane using a semi-dry blotting apparatus (BioRad, Spain). Pounceau staining of the membrane was used to check the loading. Immunoreaction was carried out using monoclonal antibody against PCNA PC10 (1:3000, Sigma-Aldrich Química, Spain) diluted in Tris-buffered saline (TBS) containing 1% (w/v) BSA and 0.1% (v/v) Tween-20. Goat anti-mouse antibody conjugated to alkaline phosphatase (1:7500, Boehringer Mannheim, Germany) was used as secondary antibody. The antigen was detected by a colorimetric assay using NBT/BCIP (Roche, Germany) following the manufacturer's protocol.

2.9. Mitotic index

The percentage of mitotic cells (mitotic index) was calculated as the ratio between mitotic cells and the number of cells scored. Following the growth curve, three replicates a day were analyzed using Hoechst 33258 staining with a fluorescence microscope (DMLS, Leica) as reported by [46]. The excitation and emission filter wavelengths were 380 nm and 410 nm, respectively.

2.10. Bimolecular fluorescence complementation

The LR reaction of the Gateway technique was used to fuse part of the Yellow Fluorescent Protein (YFP) (the N-terminal 155 amino acid or the C-terminal 84 residues) with the ORFs of *PsTrxo1* and *PsPCNA* genes in the destination vectors pE-SPYNE (N-terminal domain of YFP) and pE-SPYCE (C-terminal domain of YFP) as described in [47], generating the following constructs: 35S::*PsTrxo1-NYFP*; 35S::*PsTrxo1-CYFP*; 35S::*PsPCNA-NYFP*; 35S::*PsPCNA-CYFP*. Using the plasmid combination indicated in each case, co-bombardment of epidermal onion cells was carried out with a biolistic helium gun (DuPont PDS-1000; BioRad Laboratoires, Hercules, CA, USA) as previously described [48]. The epidermal onions were incubated in Petri dishes with sterile MS medium for 96 h in darkness at 22 °C. The fluorescence emission was analyzed after 96 h of incubation with a confocal microscope (Leica TCS-SP8) using excitation wavelengths of 405 and 458 nm and emission wavelengths of 488 and 514 nm for DAPI and YFP, respectively. The images were analyzed with a 40x objective inverter and processed using the Leica SP8 software. The results were confirmed in three biological replicates of two independent experiments.

2.11. Flow cytofluorometric analysis of the cell cycle

Cell cycle phases were determined by estimating the DNA content in TBY-2 cell nuclei using propidium iodide (50 µg/mL; PI) staining and flow cytometry analysis [49]. In order to isolate TBY-2 nuclei, protoplasts were obtained as described in [50] using 0.25% (w/v) cellulose (Sigma-Aldrich Química, Spain), 0.05% (w/v) pectolyase Y-23 (Duchefa Biochemie BV, The Netherlands) and 0.1% (v/v) pectinase (Sigma-Aldrich Química, Spain), and the progress was monitored by observing sub-samples of the cells under the light microscope. DNA profiles were examined using a flow cytometry station (MACSQuant Analyzer, Miltenyi). Histograms or density plots were arranged using the MACSQuant Digital software. For each sample, a minimum of 10,000 and a maximum of 15,000 particles were examined. Analyses were performed on three replicates in two different assays.

2.12. Measurement of reduced glutathione

The reduced glutathione (GSH) was measured with ThioStar glutathione detection reagent (L002, Arbor Assays, Ann Arbor, MI, USA) using reduced glutathione as standard (Sigma-Aldrich Química, Spain). Initially, 0.5 g of filtered cells were incubated with 5% SSA (5-sulfosalicylic acid, Sigma-Aldrich Química, Spain) with a final sample dilution in the assay of 1:20. The fluorescence was measured using excitation at 400 nm and emission at 490 nm in 96 well plates in a T-CAM.

2.13. Quantitative RT-PCR (qRT-PCR)

Total RNA was extracted using the RNeasy Plant Mini Kit (Qiagen, Germany) followed by a gel electrophoresis assay of RNA integrity. Reverse transcription (RT) was performed with 2 µg of total RNA pretreated with DNaseI (Roche, Germany) to obtain cDNA using the High-capacity cDNA Reverse Transcription Kit (Applied Biosystems, Spain) in a 20 µL reaction volume. Each cDNA sample was diluted 1:5 in sterile ddH_2O, and 1 µL of this dilution was used as template for qPCR, using a home-made 2 x SYBR Green I master mix in 10 µL reactions using the 7500 fast real-time PCR system (Applied Biosystems, Spain) according to the manufacturer's instruction. All primers used are presented in the Table S1. The cycling parameters were 95 °C for 2 min, 35 cycles of 94 °C for 15 s and 60 °C for 1 min followed by a dissociation curve running. Each gene was assayed on three biological replicates and normalized using the GAPDH cDNA levels [51].

2.14. Subcellular localization of glutathione

Double staining was performed 1, 3 and 7 days after subculture as follows: 5 µM monochlorobimane (mCBM) (Sigma-Aldrich Química, Spain) was used to detect GSH and 0.5 µM Mito-Tracker Deep-Red 633 to detect mitochondria. The cells were washed with 10 mM sodium azide (Sigma-Aldrich Química, Spain) in the cell culture medium and incubated for 5 min at 26 °C in the dark. As a negative control, 5 mM DEM (1,3-diethyl maleate) was added and left to react for two hours to inhibit the GSH signal.

2.15. Transient expression of PsTrxo1 in TBY-2 cells

The coding sequence of PsTrxo1 was amplified using the Platinum Pfx DNA Polymerase Kit (Invitrogen, Germany) with the following primers for C-terminal fusion proteins with the stop codon omitted:

attB1- PsTrxo1 AAAAAAGCAGGCTTCATGGTTGGAACCAGAAATTT

attB2-PsTrxo1 CAAGAAAGCTGGGTCGTCCTTCTTGAAGAGTTTCTC

The recognition sequences for BP Recombinase II (Invitrogen, Germany) are underlined. The PCR product was purified and cloned into the entry vector pDONR221 (Invitrogen, Germany) and sequenced. Then, the coding sequence of PsTrxo1 was subcloned with a Gateway LR recombinase into the constitutive expression vector pMDC83. *A. tumefaciens* strain GV3101 containing the plasmid pMDC83 with the construction 35S::*PsTrxo1-GFP* was transformed as described in [52] and grown in Luria-Bertani medium ($OD_{600\ nm}$ 0.8–1.1) and then TBY-2 control cells were agroinfiltrated 3 days before subcultivation at 1:40 (v/v bacteria/cells) and incubated in the dark at 26°C for 24 h. Visualization with a confocal microscopy was performed after double staining using 5 mL of cells incubated with 0.5 µM Mito-Tracker Deep-Red 633 and 10 µM DAPI (4,6-diamidino-2-phenylindole) for 10 min at room temperature in the dark.

2.16. Confocal microscopy

Confocal images were acquired using a Leica TCS-SP2 confocal laser scanning unit equipped with argon and helium-neon laser beams and attached to a Leica DM1RB inverted microscope. The excitation wavelengths for fluorochromes were 390 nm for mCBM, 364 nm for Hoechst, 633 nm for MitoTracker Deep-Red, 358 nm for DAPI and 488 nm for GFP. The emission apertures for fluorescence detection were 470–500 nm for mCBM, 380–485 for Hoechst, 630–680 nm for MitoTracker Deep Red, 440–470 for DAPI and 520–540 nm for GFP. All pictures were obtained with a of 40× objective.

2.17. Biochemical analysis of the interaction of PCNA and Trxo1 by a NADPH consumption assay

The activity of the recombinant PsTrxo1 protein was tested by the standard insulin assay where the rate of insulin reduction was measured spectrophotometrically at 650 nm as an increase in turbidity [19] using the mitochondrial electron donor, NADPH-dependent Trx reductase (AtNTRA2). Reducing activity of Trx on an oxidized PCNA was performed in 0.1 M Tris-HCl buffer pH 7.0, containing 2 mM EDTA, 0.2 mM NADPH, 50 nM AtNTRA2, 3 µM PsTrxo1 and 2 µg HsPCNA or PsPCNA. PCNA was previously oxidized with 4 mM of hydrogen peroxide for 30 min at 30 °C and dialyzed using Bio Spin6 columns (BioRad, Spain). The reaction was started by the addition of NADPH and the decrease in absorbance was followed at 340 nm at 30°C using a double beam spectrophotometer. When the reaction reached equilibrium, oxidized PCNA was added in a final total volume of 0.5 mL. Control reactions were performed on oxidized PCNA in the absence of Trxo1 and in the absence of NTR and the specificity of the reaction was tested using BSA instead of PCNA.

2.18. Redox mobility shift assay

Twenty-four micrograms of recombinant protein HsPCNA was previously reduced with 20 mM DTT in 100 µL of reaction buffer Tris-HCl 50 mM pH 7.5 during 30 min at room temperature. After eliminating the excess of DTT using a Bio-Spin 6 column (Bio-RAD, Spain), 16 µg of DTT-treated recombinant protein was oxidized in a total volume of 50 µL with 4 mM H_2O_2 for 1 h at room temperature in the reaction buffer, and afterward dialyzed using the same chromatography columns. Four micrograms of HsPCNA in 100 µL of reaction buffer Tris-HCl 50 mM pH 7.5 containing 0.2 mM NADPH were incubated with 4 µg of *PsTrxo1* and/or 0.2 µg of AtNTRA2 for one hour at 30 °C. To detect the thiol groups in the protein, cysteine derivatization by 4-acetamido-4-maleimidylstilbene-2,2-disulfonic acid (AMS, Molecular Probes, Spain) was carried out as described in [53] with some modifications. For that, 50 µL from the previous reaction were incubated with and without 10 mM AMS, 10 mM EDTA and 1% SDS in the reaction buffer in darkness for 2 h at 30 °C. The mobility was examined by non-reducing 15% SDS–PAGE using Quantity One software (BioRAD, Spain).

3. Results

3.1. PCNA interacts with PsTrxo1

Nuclear proteins were obtained after purification of nuclei from pea leaves and used in a two-dimensional electrophoresis chromatographic assay under non-reducing and reducing conditions (see Fig. 1). A mutant variant of PsTrxo1, in which Cys 37 is substituted by a Serine, was used (PsTrxo1C37) for affinity chromatography on a His-binding co-affinity resin column in order to identify the potential nuclear targets of PsTrxo1. Mass spectrometry was used to identify the major spots of soluble nuclear proteins trapped in the heterodisulfide complex formed by the mutated PsTrxo1 and the oxidized target. This analysis led to the identification of the proliferating cell nuclear antigen (PCNA) as a possible new target, among other proteins, of PsTrxo1 in the nucleus with three peptides identified in different spots, matching to the pea PCNA protein sequence (see table in Fig. 1 and Supplementary Fig. S1).

Bimolecular fluorescence complementation analysis enables direct visualization of protein interactions in living cells [47,54]. To explore whether PsTrxo1 interacts with PCNA experiments to reconstitute the YFP fluorophore were carried out, using two ORF non-fluorescent fragments of the YFP, which, when brought together by two interacting proteins fused to each of the fragments, thus reconstituting the YFP fluorophore. In this experiment the two fragments of the YFP were fused to the ORFs of *PsTrxo1* and *PsPCNA* and then co-bombarded onion epidermal cells. We also used the mutant variant PsTrxo1C37 to reach a more stable interaction with the target proteins. Microscopic observation (Fig. 2) showed that the YFP fluorescence was obtained and targeted to the nucleus with all the combinations, indicating the positive interaction in this organelle between PsTrxo1 and PsPCNA. Reconstitution of the YFP was independent of the portion of the gene used (the N-terminal or C-terminal (Fig. 2)). Nuclear DNA was stained by 4,6-diamidine-2-phenylindol (DAPI) and the fluorescence resulting from molecular association of the two YFP fragments was visualized after 36 h of incubation. As expected, no fluorescence was detected in reactions containing only one of the proteins or one of the fragments of the YFP, which were used as negative controls (see Supplementary Fig. S2).

To confirm the physical interaction of PsTrxo1 and PsPCNA a protein dot blot experiment was made, using purified recombinant proteins spotted onto nitrocellulose membranes and overlaid with both proteins separately. After extensive washing of the membrane, the presence of PCNA bound to Trxo1 spotted on the filter was revealed by anti-PCNA antibody (Fig. 3 line A) and the presence of Trxo1 bound to spotted PCNA was revealed by anti-Trxo1 (Fig. 3 line B), both being positive. As a control, PCNA protein was spotted and revealed with anti-PCNA, and the same for Trxo1 to visualize both proteins (Fig. 3 lines A, first spot and B, second spot). Also a positive control was performed in an identical membrane overlaying TBS buffer without

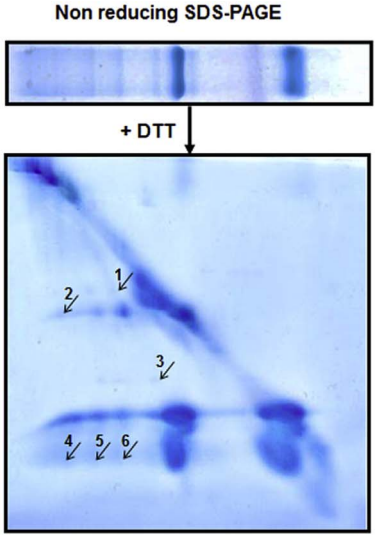

N° of spot	Sequence	Protein	Specie	BLAST[a] parameters		AC[b]	Location
				Score	e-value		
2, 4, 5, 6	VAEMGYIRYYLAPK	PCNA	*Pisum sativum*	49	$5x10^{-4}$	O82134	Nucleus
2, 3	NLSMGMNLGNMSKMLK	PCNA	*Pisum sativum*	58	$8x10^{-7}$	O82134	Nucleus
1, 3, 4, 5, 6	YMNSFTKATPLSETVTISLSSELPVVVEYK	PCNA	*Pisum sativum*	91	$8x10^{-17}$	O82134	Nucleus

[a]BLAST: *Basic Local Alignment Search Tool*, [b]Accession number Expasy http://web.expasy.org/blast/

Fig. 1. Protein pattern of pea nuclear target proteins of HisPsTrxo1C37S after affinity chromatography and 2D SDS-PAGE in non-reducing (1st dimension) and reducing (2nd dimension) conditions of the eluted complexes. Gels were stained with Blue Page[R]. Circles are drawn on the spots in which the peptides corresponding to PCNA (Proliferating Cell Nuclear Antigen) were identified by MALDI MS/MS sequencing as shown in the table. Data were combined using the BioTools program (Bruker-Daltonics) to search in the non-redundant data bases (NCBInr and SwissProt) using the Mascot (Matrix Science, UK) software. All data were manually revised using the BLAST protein program (www.expasy.org).

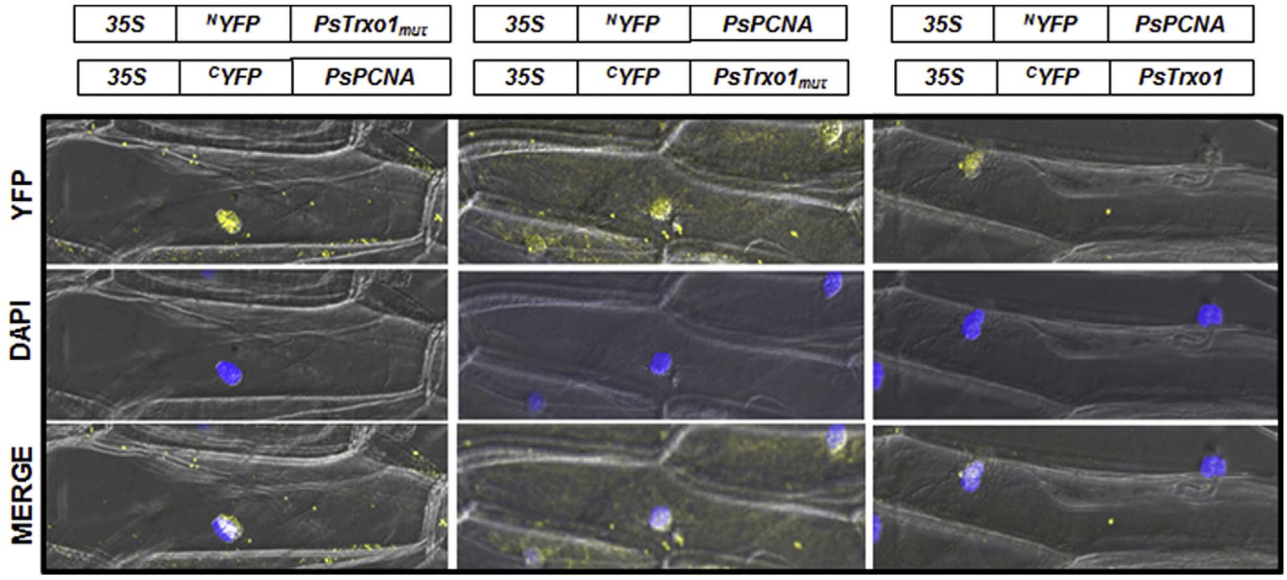

Fig. 2. Visualization of PsTrxo1 or mutated PsTrxo1$_{mut}$ and PsPCNA protein interactions in live onion cells using BiFC. Nuclear location of reconstituted yellow fluorescent protein (YFP) complexes in transiently transformed onion epidermal cells. Nuclear fluorescence was visible following reconstitution of *35S::^{N}YFP-PsTrxo1$_{mut}$* and *35S::^{C}YFP-PsPCNA*, *35S::^{N}YFP-PsPCNA* and *35S::^{C}YFP-PsTrxo1$_{mut}$* and *35S::^{N}YFP-PsPCNA* and *35S::^{C}YFP-PsTrxo1*. The fluorescence emission was analyzed after 96 h of incubation using a confocal microscope (Leica TCS-SP8) with excitation wavelengths of 405 and 458 nm and emission wavelengths of 488 and 514 nm for DAPI (nuclear stain) and YFP, respectively.

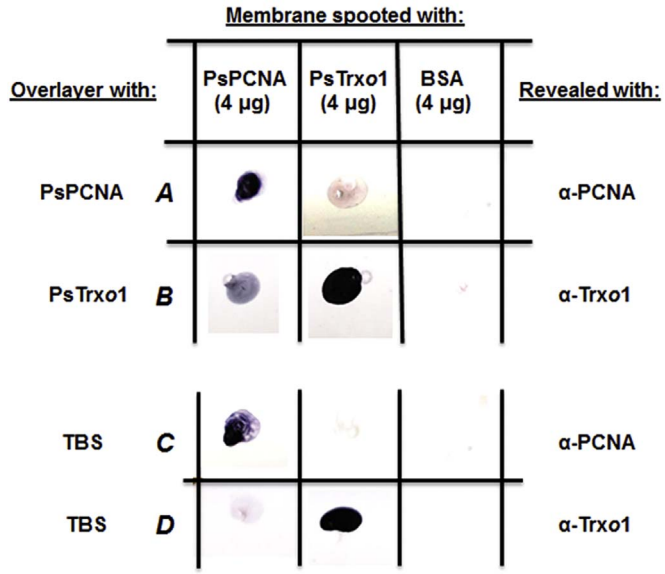

Fig. 3. Protein gel dot blot analysis of the interaction between recombinant PsPCNA and PsTrxo1. Membranes were spotted with PsPCNA, PsTrxo1 and BSA (4 µg) and were overlaid with TBS buffer containing 0.1 mg/mL recombinant PCNA and Trxo1. The presence of the proteins was revealed using anti-PCNA and anti-Trxo1 antibodies, respectively. The indicated amounts of BSA were spotted on both membranes as negative controls. TBS was used instead of the proteins to verify the antibody signals and the absence of cross-reactivity.

proteins and revealed with the corresponding antibodies (Fig. 3 line C and line D). The interaction appeared to be specific, since no signal was detected in positions corresponding to equivalent amounts of BSA, spotted as negative controls (last column in the membranes). No cross-reaction between the antibodies was noticed (lines C and D). These results confirm the physical interaction of PsTrxo1 and PsPCNA proteins.

3.2. *The NADPH thioredoxin reductase/Thioredoxin (NTR/Trx) system is able to reduce PCNA* in vitro

In order to analyse the capacity of the NTR/Trxo1 system to reduce PCNA, we initially studied how the system operates in a typical assay of Trx activity: the insulin precipitation method. For this, the reduction of the disulfide bridges of insulin was measured as an increase in the absorbance at 650 nm, indicating a loss of solubility of this protein in the presence of DTT and NTR/Trxo1 (Supplementary Fig. S3A and S3B, respectively). In this last reaction, we checked that 4′-acetamido-4′-maleimidylstilbene-2,2′-disulfonic acid (AMS), a water-soluble thiol-reactive reagent, inhibited the activity (Supplementary Fig. S3C). Afterwards, recombinant HsPCNA protein was oxidized with 4 mM H_2O_2. The reduction of oxidized Trxo1 with AtNTRA2 and NADPH was followed as a decrease in the absorbance of NADPH at 340 nm. When the reaction stabilized, oxidized PCNA was added to the reaction cuvette and a decrease in absorbance indicated the effective reduction of the HsPCNA by the NTR/Trx system (with a decrease in Abs$_{340}$/min of 0.04, Fig. 4). The same behavior was observed for PsPCNA (data not shown). Control reactions were performed in the absence of Trxo1 (with a decrease in Abs$_{340}$/min of 0.0057 in the absence and in the presence of PCNA), and in the absence of NTR (with no change in Abs$_{340}$, in the absence and in the presence of PCNA), and using BSA instead of PCNA (with no change in absorbance as shown in Fig. 4).

A parallel experiment was carried out using AMS bound to Cys residues. AMS is a NEM variant that reacts with thiols, increasing protein mass by ~0.5 kDa, so treated proteins can be analyzed by SDS-

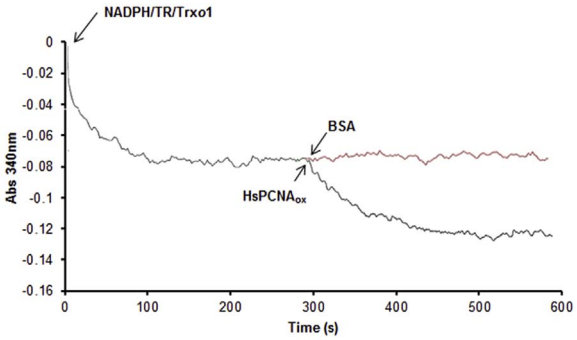

Fig. 4. Activity of NADPH-thioredoxin reductase (TR)-oxidized pea thioredoxin *o*1 (Trxo1$_{ox}$) on the reduction of oxidized HsPCNA measured by the decrease in absorbance of NADPH at 340 nm. Proteins were previously oxidized with 4 mm H_2O_2 as described in Material and Methods.

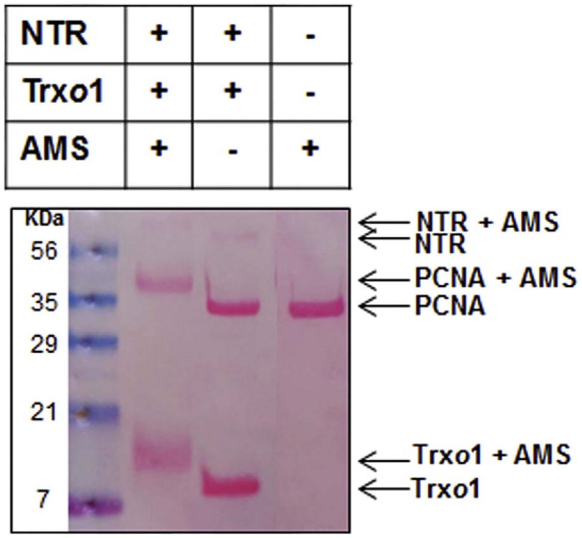

Fig. 5. Recombinant NADPH-thioredoxin reductase (AtNTRA), proliferating cell nuclear antigen (HsPCNA) and thioredoxin *o*1 (Trx*o*1) treated with or without AMS as described in Material and Methods.

PAGE. This method allows visualization of the change in electrophoretic mobility of an oxidized HsPCNA when incubated with the NTR/Trx system and AMS. As shown in Fig. 5, a shift in mobility of the HsPCNA band could correspond to the 6 Cys contained in this protein reduced by the system (lane 1 and 2). A control of oxidation is presented in lane 3 with the oxidized HsPCNA and AMS that did not change its mobility.

3.3. *Trxo1 is localized in nuclei of transformed over-expressing PsTrxo1 TBY-2 cells*

To delve further into the physiological role of Trxo1 in the nucleus, we used two TBY-2 cell culture overexpressing PsTrxo1 (Oex1 and Oex2), previously obtained as reported in [37]. Consistent with previous reports [19,37], PsTrxo1 was efficiently targeted to mitochondria and nuclei, as was observed after transient expression of exponential TBY-2 cells (3 days after subculture), with the PsTrxo1 sequence fused to GFP (in green) using Agrobacterium (Fig. 6). Images were taken with a confocal Leica microscope 24 h after agroinfiltration. DAPI blue and mitotracker Deep Red fluorescence were used as markers of nuclei and mitochondria, respectively. The over-expression of *PsTrxo1* was checked by RT-qPCR, measuring the gene level in the control and the two Oex lines after 1, 3, 5, 7 and 9 days of subculture. Gene expression was found to be stable and high in the transfected cell lines although it decreased near the end, and was undetected in control cells (Supplementary Fig. S4).

3.4. NtPCNA *and* NtTrxo1 *gene expression*

RT-qPCR was performed to measure endogenous *NtPCNA* and *NtTrxo1* gene levels during the TBY-2 control cell culture. Two PCNA genes have been described in *Nicotiana tabacum*, *PCNA1 (CAA77062)* and *PCNA2 (AAD19905)*, encoding two proteins with high level of identity (98%) containing 5 conserved cysteine residues (Cys30, Cys62, Cys81, Cys148, Cys18 [55]). The analysis of *NtTrxo1* expression in the control and overexpressing cells revealed that over-expression did not alter the endogenous levels of Trxo1 during cell culture, and this gene presented a peak of expression at day 3, decreasing thereafter, and again a slighter increase at day 6 (Fig. 7A). Interestingly, the expression of *NtPCNA* gene during the growth of the TBY-2 control line cells showed a parallel pattern until day 5, with constant low expression thereafter (Fig. 7B).

3.5. *Effect of Trxo1 over-expression on cell growth and cell cycle progression*

Cultured Tobacco Bright yellow-2 cells entered the exponential growth phase at approximately the same time (after 2 days), culture density being determined by changes in the absorbance at 600 nm. Samples were collected at 24 h intervals, with the first sample taken 24 h after the initial inoculation. As shown in Fig. 8A, the growth of the GFP control cell line and the two Trxo1 over-expressing cell lines (Oex1 and Oex2) was parallel until day 6. After this day, overexpressing lines continued growing, while the control line entered into the stationary phase, which was reached by the transformed cells at day 9 of growth (Fig. 8A).

Flow cytometry was used to assess the distribution of cells in the different phases of the cell cycle. Due to the size of plant cells and the presence of a rigid cell wall, protoplasts were obtained and used instead of whole cells. As shown in Fig. 8B, over-expression modified the percentage of cells in the different phases of the cell cycle, depending on the stage of the cell culture. After 1 and 3 days of subculture, the percentage of control cells in the GO/G1 phase remained similar (around 60%), with a similar percentage (around 16–20%). of cells in S and G2/M phases. When cell growth slowed-down (at day 7 and later), the percentage of cells in GO/G1 phase increased to around 80%, the percentage of cells in the S phase being similar (around 18%). Fewer transformed cells than control cells were found in the Go/G1 phase (between 40–65%) during cell culture, while the percentage in the S phase was higher in the first stage of the culture (although not statistically significant at around 28%) and was similar to that of control cells at 7 and 9 days, when the over-expressing cultures presented a higher cellular density. Analyzing the percentage of cells in the G2/M phases, the highest and most significant difference was observed in the final stage of the culture, when the over-expressing lines presented around 6-fold higher values than control cells.

When the percentage of TBY-2 cells undergoing mitosis was evaluated at different times during cells growth and expressed as a percentage of cells in this stage (MI: mitotic index), it was seen that the maximum percentage of mitotic cells was reached at 3 days for Oex2 line and at 4 days for the control and Oex1 line (Fig. 9). The two over-expressing lines presented a higher percentage of cells in mitosis that the control lines at both the beginning (day 1) and end (days 7 onwards) of the cell growth culture.

3.6. *Effect of Trxo1 over-expression on the PCNA protein content*

The PCNA content extracts of control and Oex PsTrxo1 TBY-2 cells, as observed by immunostaining at different days of the growth culture is provided in Fig. 10 showing a representative western of three independent experiments. PCNA level in control cells decreased when the culture reached the stationary phase to be maintained low thereafter. However, PCNA content in overexpressing cells was found higher than in control cells in these last phases, being the highest differences at days 7 and 8 of the cell growth.

3.7. *GSH content and compartmentation during TBY-2 cell proliferation*

A reduced glutathione content was recorded in the control and the two lines over-expressing PsTrxo1 (Oex1 and Oex2). As shown in Fig. 11, the GSH content decreased in the three lines as the culture progressed, with the highest content at days 1 and 3. In general, overexpressing cell lines presented a lower GSH content than the control cell line, indicating a possible compensatory mechanism between GSH and Trxo1.

To determine whether the intracellular location of GSH changes with the over-expression of PsTrxo1 in the transformed TBY-2 cells, a confocal microscopy analysis was performed during cell proliferation

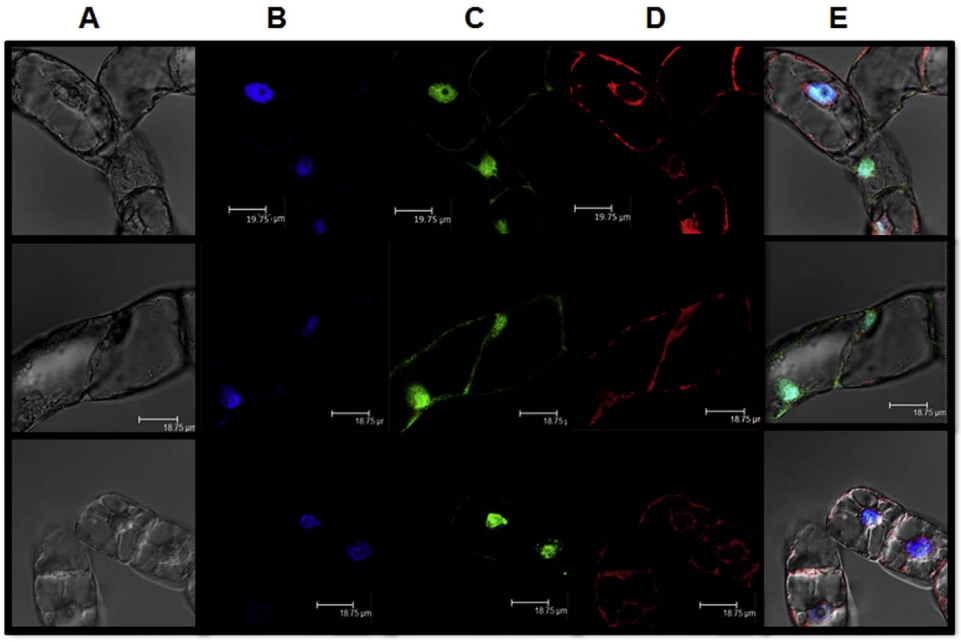

Fig. 6. Subcellular localization of PsTrx*o*1 after transient expression of PsTrx*o*1-GFP protein in TBY-2 wild type cells in the exponential phase using confocal microscopy. (A) bright field; (B) DAPI stained nucleus (blue); (C) Fluorescence of the GFP protein (green); (D) Mitotracker staining of mitochondria (red); (E) merged images. (For interpretation of the references to color in this figure legend, the reader is referred to the web version of this article.)

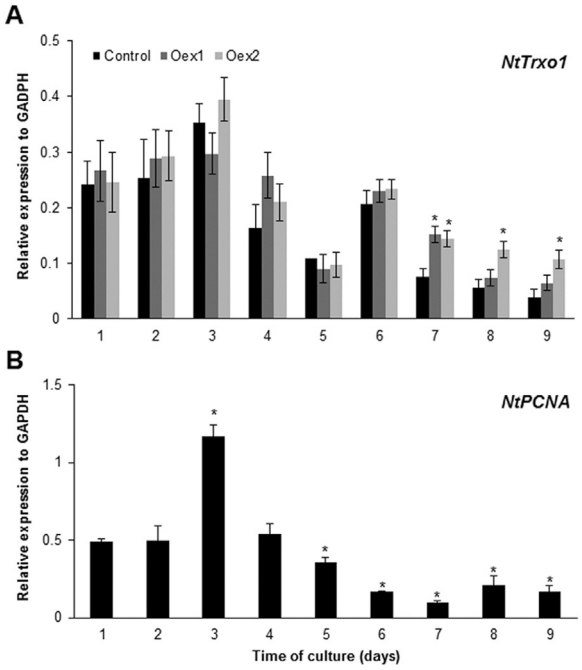

Fig. 7. (A) RT-PCR of *NtTrxo1* gene expression during the culture of control cells normalized to *GAPDH* gene expression in control and over-expressing PsTrx*o*1 lines. (B) RT-PCR of *NtPCNA* gene expression during the culture of control cells normalized to *GAPDH* gene expression. The reported values are the means of three independent experiments ± standard deviation. Asterisks indicate the values that are statistically different from the respective control (A) or the day 1 (B) (Student's *t*-test, $P < 0.05$).

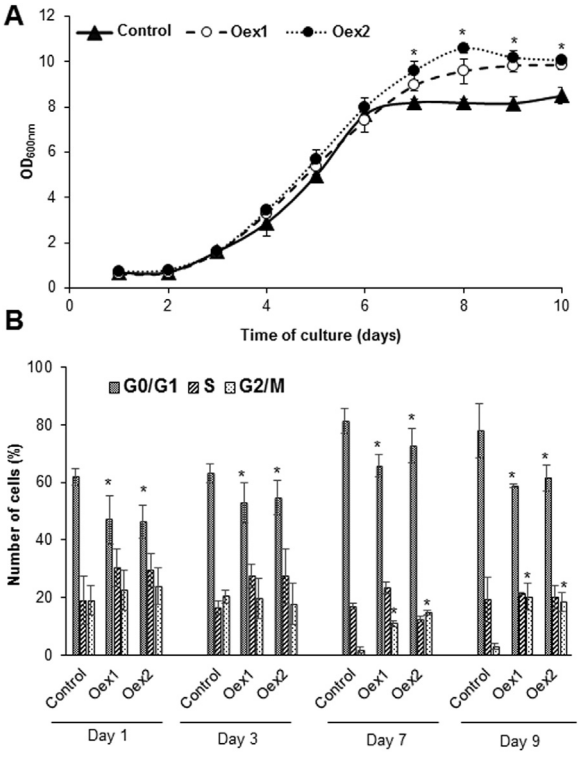

Fig. 8. (A) Effects of thioredoxin *o*1 overexpression on TBY-2 cell growth. The growth of the cell culture was monitored measuring optical density (OD) at 600 nm over time. (B) Effect of thioredoxin *o*1 overexpression on the TBY-2 cell cycle. The percentages of cells population in G0/G1, S and G2/M phases were quantified cytofluorimetrically. The reported values are the means of three independent experiments ± standard deviation. Asterisks indicate the values that are statistically different from the respective controls (Student's *t*-test, $P < 0.05$).

after 1, 3 and 8 days of subculture using monochlorobimane (mCBM) staining. As shown in Fig. 12, at day 1, GSH was located mainly in the nuclei in the three lines analyzed, while at day 3, at the beginning of the exponential phase of cell growth, fluorescence accumulation appeared to be lower in the over-expressing lines, in which a nuclear location of the GSH was still evident. The main difference was observed at day 8, when the GSH fluorescence in the nuclei was lower in the control line but remained high in both Oex lines, coinciding with the highest degree of cell density. At this stage, the percentage of cells in G2/M phase and the mitotic index was higher (see results above) than in the control cell line. Control experiments were performed *in vitro* in order to confirm the specificity of the mCBM for the thiol group of GSH and not for the

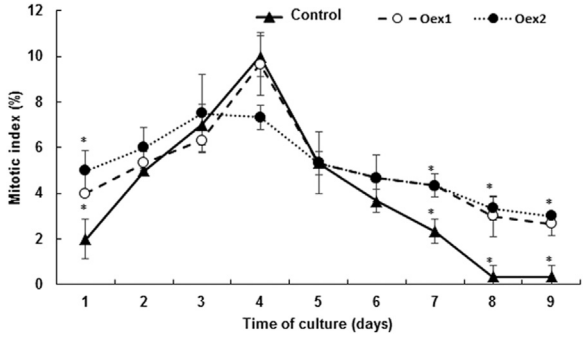

Fig. 9. Percentage of TBY-2 cells undergoing mitosis at different times during cells growth. The reported values are the means of three independent experiments ± standard deviation. Asterisks indicate the values that are statistically different from the respective controls (Student's *t*-test, $P < 0.05$).

Trxo1 ones, using recombinant PsTrxo1 and DTT-reduced PsTrxo1 proteins. As shown in Supplementary Fig. S5A, reduced Trxo1 did not react with the mCBM. As negative control we used the thiol blocking agent diethyl maleate (DEM) at 5 mM, which abolished the fluorescence signal, preventing the reaction. This experiment demonstrated that the observed fluorescence signal was specific for GSH (Supplementary Fig. S5B).

4. Discussion

4.1. PCNA as a target of PsTrxo1

In this paper, affinity column, *in vitro* and BiFC data support the idea that PsTrxo1 interacts with PCNA in the cell nucleus. At the same time, the over-expression of PsTrxo1 in TBY-2 cells correlates with changes in the growth of the culture and with the level and subcellular localization of GSH. Previous reports from our group [19] showed that in pea leaves Trxo1 is constitutively located both in mitochondria and the nucleus. Stress-induced accumulation of cytosolic Trx*h* isoforms in the nucleus has been documented by different groups in other plants [38,56]. Nuclear targets of these cytosolic/nuclear Trx*h* isoforms include proteins with antioxidant functions, such as 1-Cys Prx1, or those acting in meristematic activity gene repression, in development or cell cycle checkpoints and DNA integrity such as cyclophilin, Ran GTPase or nuclear 14.3.3 proteins [57]. On the other hand, PCNA has also been reported as a candidate target protein of Trx*h* in Medicago and in germinated barley seed embryos [58,59], although the interaction has not been conclusively demonstrated.

In the present work, after sequencing of the pea leaf nuclear proteins isolated by a proteomic affinity approach, PCNA was identified as a putative PsTrxo1 target. There is much evidence to support the conserved function and structural sequence homology of PCNA in eukaryotic organisms [see 39]. As expected, the anti-hPCNA antibody used in the *in vitro* dot blot assays was seen to recognize the pea PCNA recombinant protein and the assay allowed us to corroborate that in the

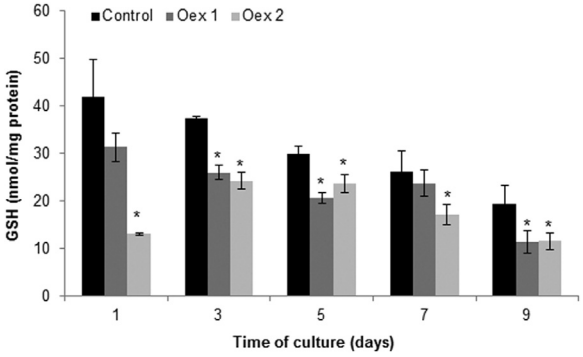

Fig. 11. Effect of thioredoxin *o*1 overexpression on the reduced glutathione content at different days of TBY-2 culture. GSH was quantified in control and two lines over-expressing PsTrxo1 (Oex1 and Oex2). The reported values are the means of three independent experiments ± standard deviation. Asterisks indicate the values that are statistically different from the respective controls (Student's *t*-test, $P < 0.05$).

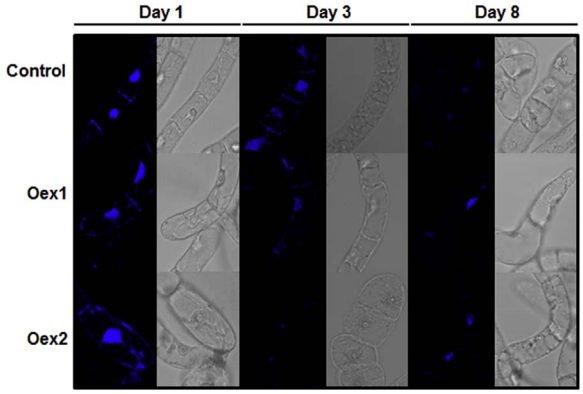

Fig. 12. Localization of GSH in control and two over-expressing PsTrxo1 TBY-2 cell lines (Oex1 and Oex2). Representative images of TBY-2 cells after 1, 3 and 8 days of growth. The fluorescence of GSH was determined with a confocal microscopy using monochlorobimane (mCBM) stain in living TBY-2 cells.

samples containing PsTrxo1 and PsPCNA incubated proteins, the protein–protein interaction was positive. Studies in yeast and animal PCNAs resulted in the identification and characterization of about 50 PCNA-interacting proteins. However, the number of identified plant PCNA-interacting proteins is very limited in comparison with human and yeast [60], and, as far as we know, its interaction with Trxs has not been previously demonstrated. It is known that biologically significant protein-protein interactions are characterized by the involvement of specific amino acid residues in the contact zones of both interaction partners. In eukaryotes, PCNA forms a homo trimeric ring structure with pseudo-6-fold symmetry, encircling the DNA helix [61,62]. The best-characterized PCNA-binding motif present in PCNA-interacting proteins is called PIP box [60]. This motif has the consensus sequence Q-xx-(h)-x-x-(a)-(a), the *h* residues having moderate hydrophobicity

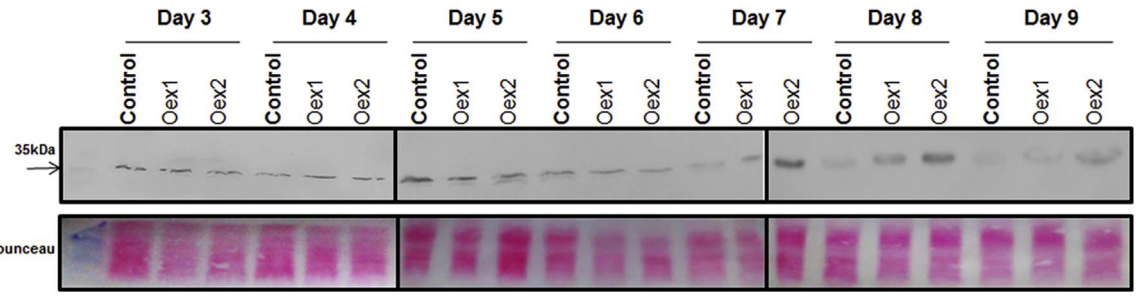

Fig. 10. PCNA protein levels by Western blot analysis in control and overexpressing (Oex1 and Oex2) PsTrxo1 TBY-2 cells at different days of the culture. A representative western is presented and the Ponceau staining shows the protein loading.

(*e.g.* M, L, I), the *a* residues having highly hydrophobic aromatic side chains (*e.g.* F, Y) and *x* being any residue [63]. PsTrxo1 presents a similar domain in its amino acid sequence (QDDSLHAIFY) [19] suggesting a possible binding motif.

We then investigated the PsTrxo1-PCNA interaction in split-yellow fluorescent protein (YFP) assays. BiFC assays significantly facilitate visualization of the subcellular sites of protein interactions under conditions that closely reflect the normal physiological environment [47]. Localization results from a previous study using GFP coupled to Trxo1 [19] and the results for the co-transformed proteins in the present BiFC analysis point to identical compartments in the nucleus. This confirmation underlines the significance of the results obtained by BiFC interactions, and lends additional physiological support to the PsTrxo1-PCNA interaction in the nucleus.

Recently, numerous studies have focused on PCNA post-translational modification and its implication for DNA replication and repair. Such multiple post-translational modifications, including acetylation, methylation, phosphorylation, sumoylation, ubiquitylation and *S*-nitrosylation, regulate the PCNA function [64,65]. As an example, a recent study on the *S*-nitrosylation status of PCNA in SH-SY5Y cells treated with rotenone, used as a model of neuronal death, identified the two-cysteine residues, PCNA-Cys^{81} and Cys^{162}, as candidate *S*-nitrosylated residues. The *S*-nitrosylation of PCNA-Cys^{81} affected the interaction between PCNA and caspase-9, which may act as a mediator in the apoptotic pathway [66]. However no redox modification on these Cys residues by non-radical oxidants, including peroxides, was reported. In photosynthetic eukaryotes, PCNA harbors five cysteines in each monomer although one of these cysteines is not essentially conserved in Arabidopsis [67]. Specifically in *Pisum sativum* and *Nicotiana tabacum*, one and two PCNA proteins were described respectively, with a high level of amino acid sequence identity (97%) in the two tobacco proteins. In both isoforms, 5 conserved cysteine residues have been described whereas human PCNA contains 6 cysteine residues [39].

We previously proposed that one of the PsTrxo1 functions in the mitochondria and nucleus of pea and TBY-2 cells is to offer protection against ROS, mainly H_2O_2. This antioxidant role would allow PsTrxo1 to control the redox status of mitochondrial and nuclear proteins in pea leaves and tobacco cells [37,68]. Thus, in mitochondria, the Trxo1 function has been related with redox regulation of proteins, including the respiratory alternative oxidase component (AOX, [19,69] and with the detoxification of ROS *via* mitochondrial peroxiredoxin (PrxIIF)) [2].

In the nucleus, Trxo1 may also be acting as a component of ROS scavenging systems, preventing deleterious effects of nuclear ROS accumulation. Since our results confirmed that PCNA is one of the PsTrxo1 nuclear target proteins, we next tested whether PsTrxo1 is involved in the reduction of an oxidized PCNA upon H_2O_2 treatment. *In vitro* classical disulfide reductase Trxo1 activity assays demonstrated that the NAD(P)H/AtNTRA2/PsTrxo1 system efficiently reduced oxidized HsPCNA.

4.2. Effect of PsTrxo1 overexpression in TBY-2 cells

Another factor analyzed in this work is the effect of PsTrxo1 overexpression in TBY-2 cells on the dynamic of the growth of the culture, as a process related to the cell cycle. Importantly, the maintenance of a nuclear and mitochondrial PsTrxo1 localization in overexpressing cells was confirmed, as previously reported by western-blot analysis [37]. In the present study this is corroborated by transient expression analysis of YFP fusions in agroinfiltrated TBY-2 cells. YFP-fusion analysis found Trxo1 to be mainly located in the nucleoplasm, which agrees with our previous findings in pea leaves [19]. Recently, we reported that the over-expression of PsTrxo1 in TBY-2 cells increased cell viability in an oxidative situation induced by H_2O_2 treatment. A decreased content of endogenous H_2O_2 might be responsible, at least in part, for the delayed cell death found in PsTrxo1 overexpressing cells, in which changes in oxidative parameters and antioxidants were less extensive after oxidative treatment.

Here, as a first step, we observed that in TBY-2 cells, endogenous *NtPCNA* gene expression levels were very similar to the level of endogenous *NtTrxo1*, both being high in the early stages of cell growth (day 1), peaking at the beginning of the exponential growth phase (day 3), and decreasing during the advanced growth period (stationary phase) (days 7, 8 and 9). PCNA is a well-known molecular marker for cell proliferation because of its role in replication, and its expression pattern in TBY-2 cells agrees with that role and with observations reported in plants, where the PCNA genes were actively expressed during intensive cell proliferation [55,70]. Moreover, in *Catharanthus roseus* cells, PCNA expression was mainly confined to the S phase of the cell cycle, providing direct proof that its expression correlates with cell proliferation and DNA replication [71].

In this context, cellular DNA synthesis and cell growth depend on the production of an adequate and balanced supply of deoxyribonucleotides. In mammalian cells the activity of RNR, a key enzyme for deoxyribonucleotide synthesis, is cell cycle-dependent and Trx and Grx are well-known regulators of DNA replication through their involvement in the catalytic mechanism of this enzyme [72]. Proliferating cells require a large amount of deoxyribonucleotides during the S phase of the cell cycle [73] and it has been reported that low cell-culture density, which is associated with oxidation of thiols and increased cell proliferation, affects the localization of Trx1 in animal cell cultures, promoting its translocation to the nucleus [6]. On the other hand, Trx has been involved in the regulation of the cell cycle in the G1 to S phase and, in fact, the expression of human Trx is highest in the early S phase [74]. Other evidence pointing to the involvement of Trx in cell cycle progression was obtained in yeast, where the absence of *Trx1 and Trx2* genes slowed down the rate of DNA replication and inhibited the normal progress of cell reproduction [75]. Therefore, the correlation found between endogenous Trxo1 and PCNA expression during TBY-2 cell culture seems to provide additional proof of the involvement of both proteins in S-phase replication, in agreement with previous reports, and suggests the existence of a common gene-regulatory mechanism. Furthermore, the data presented also indicated that as culture progressed, overexpressing Trxo1 lines maintained higher PCNA protein amounts than non-overexpressing lines, the differences depending on the time of the culture and interestingly when a higher proliferation and/or mitotic index is occurring. This indicates a positive effect of Trxo1 on PCNA which could be linked to PCNA activity. Related with that, we have obtained preliminary results indicating a possible PCNA redox change during the progression of the cell culture. That is a new and interesting aspect that merits further investigation and will be an object of a deeper study in our laboratory.

The data presented here show that the differences found in the overexpressing cells closely resembled the changes in the glutathione pool, which, in turn, were similar to those reported in mammalian and plant cells [42,76] where the glutathione content gradually decreased toward the end of the exponential growth phase, reaching the lowest values during the stationary phase of cell culture. This glutathione decrease was, in general, more intense in both PsTrxo1 overexpressing lines, even in the advanced growth phases (days 7–9), when the percentage of cells in the G2/M phase was higher than in non-overexpressing cells; at the same time, nuclear chromatin is duplicated and the cells enter into mitosis, as deduced from the observed higher mitotic index. It has recently been reported that the levels of two cytosolic *h*-type Trxs *TH7* and *TH8* mRNAs greatly increased in GSH depleted *rml1-1* Arabidopsis mutants [77]. The transcriptome profile of these mutants showed an inverse relation between GSH availability and Trx expression, which resembles our Trxo1 and glutathione results in the overexpressing Trxo1 cell lines. It appears that thioredoxin overexpression could be compensated by a decrease in GSH levels, underscoring the importance of a balanced redox environment for cells

to proliferate. Similarly, in yeast double mutants, the reduced cytoplasmic *Trx1* and *Trx2* was reported to produce an increase in the total glutathione content by means of an unknown underlying mechanism adjusting glutathione levels in response to thioredoxin deficiency [30].

Cellular redox homeostasis is crucial for cell proliferation and glutathione is a key component of this regulation in plant and animal cells [42,78]. Recent evidence has shown that GSH is sequestered in the nucleus in the early stages of the cell cycle, a fact which appears to have a critical regulatory role as the cell cycle progresses. However, no GSH accumulation was found in the nucleus of cells in the quiescent GO phase [80,81]. GSH was also observed in the nuclei of the dividing pericycle cells following activation to form the lateral root meristem. These results suggest a dynamic regulation of the nuclear GSH pool during the cell cycle [79].

In the present work, data concerning the sub-cellular localization of GSH suggest that in the early phases of cell growth, when cells are entering the exponential phase (day 3), at least part of the glutathione pool was located in the nucleus in its reduced form (GSH) and that a similar proportion of the pool was thus located in non-overexpressing and overexpressing lines, although GSH levels were lower and Trx levels were higher in the nucleus in both Trx*o*1 overexpressing cells. However, in non-overexpressing cells in an advanced growth phase when cells reached the stationary phase (day 8), nuclear GSH was practically undetectable, whereas such a decrease in nuclear GSH did not occur with the same intensity in over-expressing Trx*o*1 lines, which maintained similar levels to those at day 3. Clearly more information is needed in order to explain the changes in nuclear GSH levels and the potential compensatory role of Trx. These data on nuclear GSH agree with previous reports in Arabidopsis, tobacco and fibroblast cell cultures [79–81], indicating that the localization of glutathione is determined by the stage of the cell cycle. Thus, in overexpressing TBY-2 cells, the retained GSH level in the nucleus seems to be necessary for the active division phases (G2/M) to occur, even in advanced stages of growth in overexpressing cells. Interestingly, in rml1-1 *Arabidopsis* mutants [77], transcript data also demonstrated that redox regulation involving GSH is important for the genes encoding CYCs, CDKs and PCNA that control the G2 to M transition.

5. Conclusions

As a summary, in the TBY-2 cell nucleus, Trx*o*1, besides its effect on cell proliferation and cell cycle progression, may provide, together with GSH, the reductive environment required to protect DNA against oxidation during replication. However this suggestion needs to be confirmed in future studies. As we have also previously described, another Trx*o*1 function in the nucleus may be its involvement in DNA synthesis and repair through its interaction with PCNA. Although there is no evidence of a redox regulation of PCNA *in vivo,* our present data point to a higher amount of PCNA protein in overexpressing Trx*o*1 lines in the growth phases when differences in the mitotic index and the percentage of cells in S-G2/M phases were particularly evident. This may be a reflection of a functional link between both proteins. In this sense, further biochemical studies have being initiated in order to clarify the possible *in vivo* PCNA redox regulation by Trx*o*1. Moreover the relation between such possible redox PCNA regulation and nuclear GSH levels need to be clarified. These investigations are necessary to provide insight into the role of redox regulation in key aspects of cell cycle plant biology.

Author contributions

A.J., F.S. F.V.P. and P.C. designed the research; A.C, A. O-E, and R. I-F., performed the experiments; A.C, A. O-E., F.S. and A.J. analyzed the data; A.J., F.V.P. and F.S. wrote the paper.

Conflict of interests

The authors declare no conflict of interest.

Funding sources

This study was supported by the Spanish grants MINECO-BFU/FEDER 2014-52452-P, PROMETEOII/2014/056 Generalitat Valenciana and Seneca Foundation Excellence Project 19876/GERM/15 and MICINN-CONSOLIDER CSD2007-00057.

Acknowledgments

The authors thank Dr. J.J. Lázaro (EEZ-CSIC, Granada) for the kind gift of AtNTRA protein, Dr. E. Olmos (CEBAS-CSIC, Murcia) for his advice and valuable suggestions on the TBY-2 cell culture, the technician Isabel Esmorís and the PhD students Santiago Ibañez-Cabellos and Marta Seco (University of Valencia) for their valuable assistance in gene expression and glutathione analysis and Dr. T. Philip for correction of the written English in the manuscript.

Appendix A. Supplementary material

Supplementary data associated with this article can be found in the online version at http://dx.doi.org/10.1016/j.redox.2017.01.018.

References

[1] R. Mittler, S. Vanderauwera, N. Suzuki, G. Miller, V.B. Tognetti, K. Vandepoele, M. Gollery, V. Shulaev, F. Van Breusegem, ROS signaling: the new wave?, Trends Plant Sci. 16 (2011) 300–309.
[2] J.J. Lázaro, A. Jiménez, D. Camejo, I. Iglesias-Baena, M.C. Martí, A. Lázaro-Payo, S. Barranco-Medina, F. Sevilla, Dissecting the integrative antioxidant and redox systems in plant mitochondria. Effect of stress and S-nitrosylation, Front. Plant Sci. 4 (2013) 1–20.
[3] C. Mata-Pérez, J.C. Begara-Morales, M. Chaki, B. Sánchez-Calvo, R. Valderrama, M.N. Padilla, F.J. Corpas, J.B. Barroso, Protein tyrosine nitration during development and abiotic stress response in plants, Front. Plant Sci. 7 (2016) 1699.
[4] C.H. Foyer, G. Noctor, Redox sensing and signalling associated with reactive oxygen in chloroplasts, peroxisomes and mitochondria, Physiol. Plant 119 (2003) 355–364.
[5] M. Rodriguez-Serrano, M.C. Romero-Puertas, M. Sanz-Fernandez, J. Hu, L.M. Sandalio, Peroxisomes extend peroxules in a fast response to stress via a reactive oxygen species-mediated induction of peroxin PEX11a, Plant Physiol. (2016). http://dx.doi.org/10.1104/pp.16.00648.
[6] Y.M. Go, D.P. Jones, Redox control systems in the nucleus: mechanisms and functions, Antioxid. Redox Signal. 13 (2010) 489–509.
[7] C. Ashtamker, V. Kiss, M. Sagi, O. Davydov, R. Flu, Diverse subcellular locations of cryptogenin-induced reactive oxygen species production in tobacco bright yellow- 2 cells, Plant Physiol. 143 (2007) 1817–1826.
[8] K. Apel, H. Hirt, Reactive oxygen species: metabolism, oxidative stress, and signal transduction, Annu. Rev. Plant Biol. 55 (2004) 373–399.
[9] M.C. de Pinto, V. Locato, L. De Gara, Redox regulation in plant programmed cell death, Plant Cell Environ. 35 (2012) 234–244.
[10] R. González, M.J. López-Grueso, J. Muntané, J.A. Bárcena, A.C. Padilla, Redox regulation of metabolic and signaling pathways by thioredoxin and glutaredoxin in NOS-3 overexpressing hepatoblastoma cells, Redox Biol. 6 (2015) 122–134.
[11] S. Boronat, A. Doménech, E. Hidalgo, Proteomic characterization of reversible thiol oxidations in proteomes and proteins, Antioxid. Redox Signal (2016). http://dx.doi.org/10.1089/ars.2016.6720.
[12] D. Camejo, M.C. Romero-Puertas, M. Rodríguez-Serrano, L.M. Sandalio, J.J. Lázaro, A. Jiménez, F. Sevilla, Salinity-induced changes in *S*-nitrosylation of pea mitochondrial proteins, J. Proteom. 79 (2013) 87–99.
[13] C.H. Foyer, G. Noctor, Redox signaling in plants, Antioxid. Redox Signal. 18 (2013) 2087–2090.
[14] F. Sevilla, D. Camejo, A. Ortiz-Espín, A. Calderón, J.J. Lázaro, A. Jiménez, Thioredoxin/peroxiredoxin/sulfiredoxin system: current overview on its redox function in plants and regulation by ROS and RNS, J. Exp. Bot. 66 (2015) 2945–2955.
[15] F. Sevilla, A. Jiménez, J.J. Lázaro, What do the plant mitochondrial antioxidant and redox systems have to say in salinity, drought and extreme temperature abiotic stress situations? in: Dharmendra K. Gupta et al. (Eds.): Reactive Oxygen Species and Oxidative Damage in Plants Under Stress, pp. 23–55, doi: ⟨10.1007/879-3-319-20421-5-2⟩, 2015.
[16] Y. Meyer, C. Belin, V. Delorme-Hinoux, J.P. Reichheld, C. Riondet, Thioredoxin and glutaredoxin systems in plants: molecular mechanisms, crosstalks, and

functional significance, Antioxid. Redox Signal. 17 (2012) 1124–1160.
[17] C.H. Lillig, A. Holmgren, Thioredoxin and related molecules-from biology to health and disease, Antioxid. Redox Signal. l9 (2007) 25–47.
[18] C. Laloi, N. Rayapuram, Y. Chartier, J.M. Grienenberger, G. Bonnard, Y. Meyer, Identification and characterization of a mitochondrial thioredoxin system in plants, Proc. Natl. Acad. Sci. USA 98 (2001) 14144–14149.
[19] M.C. Martí, E. Olmos, J.J. Calvete, I. Díaz, S. Barranco-Medina, J. Whelan, J.J. Lázaro, F. Sevilla, A. Jiménez, Mitochondrial and nuclear localization of a novel pea thioredoxin: identification of its mitochondrial target proteins, Plant Physiol. 150 (2009) 646–657.
[20] P. Pulido, R. Cazalis, F.J. Cejudo, An antioxidant redox system in the nucleus of wheat seed cells suffering oxidative stress, Plant J. 57 (2009) 132–145.
[21] C. Marchal, V. Delorme-Hinoux, L. Bariat, W. Siala, C. Belin, J. Saez-Vasquez, C. Riondet, J.P. Reichheld, NTR/NRX define new thioredoxin system in the nucleus of *Arabidopsis thaliana* cells, Mol. Plant 7 (2014) 30–44.
[22] F.J. Cejudo, A.J. Meyer, J.P. Reichheld, N. Rouhier, J.A. Traverso, Thiol-based redox homeostasis and signaling, Front. Plant Sci. 5 (2014) 266.
[23] K. Hirota, M. Murata, Y. Sachi, H. Nakamura, J. Takeuchi, K. Mori, J. Yodoi, Distinct roles of thioredoxin in the cytoplasm and in the nucleus. A two-step mechanism of redox regulation of transcription factor NF-kB, J. Biol. Chem. 274 (1999) 27891–27897.
[24] X.P. Chen, S. Liu, W.X. Tang, Z.W. Chen, Nuclear thioredoxin-1 is required to suppress cisplatin-mediated apoptosis of MCF-7 cells, Biochem. Biophys. Res. Commun. 361 (2007) 362–366.
[25] Z. Mou, W. Fan, X. Dong, Inducers of plant systemic acquired resistance regulate NPR1 function through redox changes, Cell 113 (2003) 935–944.
[26] M.K. Jensen, T. Kjaersgaard, N.M. Nielsen, P. Galberg, K. Petersen, C. O'Shea, K. Skriver, The *Arabidopsis thaliana* NAC transcription factor family: structure–function relationships and determinants of ANAC019 stress signalling, Biochem. J. 426 (2010) 183–196.
[27] J. Chiu, I.W. Dawes, Redox control of cell proliferation, Trends Cell Biol. 22 (2012) 592–601.
[28] T.C. Laurent, E.C. Moore, P. Reichard, Enzymatic synthesis of deoxyribonucleotides, IV: isolation and characterization of thioredoxin, the hydrogen donor from *Escherichia coli* B, J. Biol. Chem. 239 (1964) 3436–3444.
[29] H. Hartman, M. Wu, B.B. Buchanan, J.C. Gerhart, Spinach thioredoxin m inhibits DNA synthesis in fertilized *Xenopus* eggs, Proc. Natl. Acad. Sci. USA 90 (1993) 2271–2275.
[30] E.G.D. Muller, A glutathione reductase mutant of yeast accumulates high levels of oxidized glutathione and requires thioredoxin for growth, Mol. Cell. Biol. 37 (1996) 1805–1813.
[31] F.Z. Avval, A. Holmgren, Molecular mechanisms of thioredoxin and glutaredoxin as hydrogen donors for mammalian S-phase ribonucleotide reductase, J. Biol. Chem. 284 (2009) 8233–8240.
[32] A. Koc, C.K. Mathews, L.J. Wheeler, M.K. Gross, G.F. Merrill, Thioredoxin is required for deoxyribonucleotide pool maintenance during S phase, J. Biol. Chem. 281 (2006) 15058–15063.
[33] N. Wakasugi, Y. Tagaya, H. Wakasugi, A. Mitsui, M. Maeda, J. Yodoi, T. Tursz, Adult T-cell leukemia-derived factor thioredoxin, produced by both human T-lymphotropic virus type I- and Epstein-Barr virus-transformed lymphocytes, acts as an autocrine growth factor and synergizes with interleukin 1 and interleukin 2, Proc. Natl. Acad. Sci. USA 87 (1990) 8282–8286.
[34] J.P. Reichheld, K. Mehdi, C. Riondet, M. Droux, G. Bonnard, Y. Meyer, Inactivation of thioredoxin reductases reveals a complex interplay between thioredoxin and glutathione pathways in Arabidopsis development, Plant Cell 19 (2007) 1851–1865.
[35] W. García-Giménez, J.L. Markovic, F. Dasí, G. Queval, D. Schnaubelt, C.H. Foyer, F.V. Pallardó, Nuclear glutathione, Biochim. Biophys. Acta 1830 (2013) 3304–3316.
[36] B. Zechmann, F. Mauch, L. Sticher, M. Müller, Subcellular immunocytochemical analysis detects the highest concentrations of glutathione in mitochondria and not in plastids, J. Exp. Bot. 59 (2008) 4017–4027.
[37] A. Ortiz-Espín, V. Locato, D. Camejo, A. Schiermeyer, L. De Gara, F. Sevilla, A. Jiménez, Over-expression of Trxo1 increases the viability of tobacco BY-2 cells under H_2O_2 treatment, Ann. Bot. 116 (2015) 571–582.
[38] V. Delorme-Hinoux, S.A. Bangash, A.J. Meyer, J.P. Reichheld, Nuclear thiol redox systems in plants, Plant Sci. 243 (2016) 84–95.
[39] W. Strzalka, A. Ziemienowicz, Proliferating cell nuclear antigen (PCNA): a key factor in DNA replication and cell cycle regulation, Ann. Bot. 107 (2011) 1127–1140.
[40] T. Yamamoto, Y. Mori, T. Ishibashi, Y. Uchiyama, T. Ueda, T. Ando, J. Hashimoto, S. Kimura, K. Sakaguchi, Interaction between proliferating cell nuclear antigen (PCNA) and a DnaJ induced by DNA damage, J. Plant Res. 118 (2005) 91–97.
[41] T. Nagata, Y. Nemoto, S. Hasezawa, Tobacco BY-2 Cell Line as the "HeLa" Cell in the Cell Biology of Higher Plants, Int. Rev. Cytol. 132 (1992) 1–30.
[42] T.K. Pellny, V. Locato, P.D. Vivancos, J. Markovic, L. De Gara, F.V. Pallardó, C.H. Foyer, Pyridine nucleotide cycling and control of intracellular redox state in relation to poly (ADP-ribose) polymerase activity and nuclear localization of glutathione during exponential growth of Arabidopsis cells in culture, Mol. Plant. 2 (2009) 442–456.
[43] M.M. Bradford, A rapid and sensitive method for the quantification of microgram quantities of protein utilizing the principle of protein–dye binding, Anal. Biochem. 72 (1976) 248–254.
[44] D. Suckau, A. Resemann, M. Schuerenberg, P. Hufnagel, J. Franzen, A. Holle, A novel MALDI LIFT-TOF/TOF mass spectrometer for proteomics, Anal. Bioanal. Chem. 376 (2003) 952–965.
[45] U.K. Laemmli, Cleavage of structural proteins during the assembly of the head of bacteriophage T4, Nature 227 (1970) 680–685.
[46] V. Houot, P. Etienne, A.S. Petitot, S. Barbier, J.P. Blein, L. Suty, Hydrogen peroxide induces programmed cell death features in cultured tobacco BY-2 cells in a dose-dependent manner, J. Exp. Bot. 52 (2001) 1721–1730.
[47] M. Walter, C. Chaban, K. Schütze, O. Batistic, K. Weckermann, C. Näke, D. Blazevic, C. Grefen, K. Schumacher, C. Oecking, K. Harter, J. Kudla, Visualization of protein interactions in living plant cells using bimolecular fluorescence complementation, Plant J. 40 (2004) 428–438.
[48] I. Díaz, J. Vicente-Carbajosa, Z. Abraham, M. Martínez, I. IsabelLamoneda, P. Carbonero, The GAMYB protein from barley interacts with the DOF transcription factor BPBF and activates endosperm-specific genes during seed development, Plant J. 29 (2002) 453–464.
[49] J. Fried, A.G. Perez, B.D. Clarkson, Flow cytofluorometric analysis of cell cycle distributions using propidium iodide. Properties of the method and mathematical analysis of the data, J. Cell Biol. 71 (1976) 172–181.
[50] V. Locato, M.C. de Pinto, L. De Gara, Different involvement of the mitochondrial, plastidial, and cytosolic ascorbate–glutathione redox enzymes in heat shock responses, Physiol. Plant. 135 (2009) 296–306.
[51] T. Czechowski, M. Stitt, T. Altmann, M.K. Udvardi, W. Scheible, Genome-wide identification and testing of superior reference genes for transcript normalization in Arabidopsis, Plant. Physiol. 139 (2005) 5–17.
[52] R. Nagel, A. Elliott, A. Masel, R.G. Birch, J.M. Manners, Electroporation of binary Ti plasmid vector into *Agrobacterium tumefaciens* and *Agrobacterium rhizogenes*, FEMS Microbiol. Lett. 67 (1990) 325–328.
[53] B. Biteau, J. Labarre, M.B. Toledano, ATP-dependent reduction of cysteine–sulphinic acid by *S. cerevisiae* sulphiredoxin, Nature 425 (2003) 980–984.
[54] I. Diaz, M. Martínez, I. La Moneda, I. Rubio-Somoza, P. Carbonero, The DOF protein, SAD, interacts with GAMYB in plant nuclei and activates transcription of endosperm-specific genes during barley seed development, Plant J. 42 (2005) 652–662.
[55] W. Strzalka, A. Kaczmarek, B. Naganowska, A. Ziemienowicz, Identification and functional analysis of PCNA1 and PCNA-like1 genes of *Phaseolus coccineus*, J. Exp. Bot. 61 (2010) 873–888.
[56] A. Serrato, J. Crespo, F. Florencio, F. Cejudo, Characterization of two thioredoxins h with predominant localization in the nucleus of aleurone and scutellum cells of germinating wheat seeds, Plant M. Biol. 46 (2001) 361–371.
[57] W. Strzalka, C. Aggarwal, *Arabidopsis thaliana* proliferating cell nuclear antigen 1 and 2 possibly form homo- and hetero-trimeric complexes in the plant cell, Plant Signal. Behav. 8 (2013) e24837.
[58] F. Alkhalfioui, M. Renard, W.H. Vensel, J. Wong, C.K. Tanaka, W.J. Hurkman, B.B. Buchanan, F. Montrichard, Thioredoxin-linked proteins are reduced during germination of *Medicago truncatula* seeds, Plant Physiol. 144 (2007) 1559–1579.
[59] P. Hägglund, J. Bunkenborg, K. Maeda, B. Svensson, Identification of thioredoxin disulfide targets using a quantitative proteomics approach based on isotope-coded affinity tags, J. Prot. Res. 7 (2008) 5270–5276.
[60] J.B. Vivona, Z. Kelman, The diverse spectrum of sliding clamp interacting proteins, FEBS Lett. 546 (2003) 167–172.
[61] J.M. Gulbis, Z. Kelman, J. Hurwitz, M. O'Donnell, J. Kuriyan, Structure of the C-terminal region of p21 (WAF1/CIP1) complexed with human PCNA, Cell 87 (1996) 297–306.
[62] W. Strzalka, T. Oyama, K. Tori, K. Morikawa, Crystal structures of the Arabidopsis thaliana proliferating cell nuclear antigen 1 and 2 proteins complexed with the human p21C-terminal segment, Prot. Sci. 18 (2009) 1072–1080.
[63] G. Maga, U. Hübscher, Proliferating cell nuclear antigen (PCNA): a dancer with many partners, J. Cell Sci. 116 (2003) 3051–3060.
[64] W. Strzalka, P. Labecki, F. Bartnicki, C. Aggarwal, M. Rapala-Kozik, C. Tani, K. Tanaka, H. Gabrys, *Arabidopsis thaliana* proliferating cell nuclear antigen has several potential sumoylation sites, J. Exp. Bot. 63 (2012) 2971–2983.
[65] H.D. Ulrich, T. Takahashi, Readers of PCNA modifications, Chromosoma 122 (2013) 259–274.
[66] L. Yin, Y. Xie, S. Yin, X. Lv, J. Zhang, Z. Gu, H. Sun, S. Liu, The S-Nitrosylation status of PCNA localized in cytosol impacts the apoptotic pathway in a Parkinson's disease paradigm, PLoS One 10 (2015) e0117546. http://dx.doi.org/10.1371/journal.pone.0117546.
[67] W. Strzalka, A. Ziemienowicz, Molecular cloning of *Phaseolus vulgaris* cDNA encoding proliferating cell nuclear antigen, J. Plant Physiol. 164 (2007) 209–213.
[68] M.C. Martí, I. Florez-Sarasa, D. Camejo, M. Ribas-Carbó, J.J. Lázaro, F. Sevilla, A. Jiménez, Response of the mitochondrial antioxidant redox system and respiration to salinity in pea plants, J. Exp. Bot. 62 (2011) 3863–3874.
[69] E. Gelhaye, N. Rouhier, J. Gerard, Y. Jolivet, J. Gualberto, N. Navrot, P. Ohlsson, G. Wingsle, M. Hirasawa, D.B. Knaff, H. Wang, P. Dizengremel, Y. Meyer, J.P. Jacquot, A specific form of thioredoxin *h* occurs in plant mitochondria and regulates the alternative oxidase, Proc. Natl. Acad. Sci. USA 101 (2004) 14545–14550.
[70] S. Kimura, T. Suzuki, Y. Yanagawa, T. Yamamoto, H. Nakagawa, I. Tanaka, J. Hashimoto, K. Sakaguchi, Characterization of plant proliferating cell nuclear antigen (PCNA) and flap endonuclease-1 (FEN-1), and their distribution in mitotic and meiotic cell cycles, Plant J. 28 (2001) 643–653.
[71] H. Kodama, M. Ito, N. Ohnishi, I. Suzuka, A. Komamine, Molecular cloning of the gene for plant proliferating-cell nuclear antigen and expression of this gene during the cell cycle in synchronized cultures of *Catharanthus roseus* cells, Eur. J. Biochem. 197 (1991) 495–503.
[72] F. Aslund, B. Ehn, A. Miranda-Vizuete, C. Pueyo, A. Holmgren, Two additional glutaredoxins exist in *Escherichia coli*: glutaredoxin 3 is a hydrogen donor for ribonucleotide reductase in a thioredoxin/glutaredoxin 1 double mutant, Proc. Nat.

Acad. Sci. USA 91 (1994) 9813–9817.
[73] R. SenGupta, A. Holgrem, Thioredoxin and glutaredoxin-mediated redox regulation of ribonucleotide reductase, World J. Biol. Chem. 5 (2014) 68–74.
[74] M. Mochizuki, Y.W. Kwon, J. Yodoi, H. Masutani, Thioredoxin Regulates Cell Cycle via the ERK1/2-Cyclin D1 Pathway, Antioxid. Redox Signal. 11 (2009) 2957–2971.
[75] E.G.D. Muller, Thioredoxin deficiency in yeast prolongs S phase and shortens the G1 interval of the cell cycle, J. Biol. Chem. 266 (1991) 9194–9201.
[76] J. Markovic, C. Borrás, A. Ortega, J. Sastre, J. Viña, F.V. Pallardó, Glutathione is recruited into the nucleus in early phases of cell proliferation, J. Biol. Chem. 282 (2007) (2007) 20416–20424.
[77] D. Schnaubelt, G. Queval, Y. Dong, P. Díaz-Vivancos, M.E. Makgopa, G. Howell, A. De Simone, J. Bai, M.A. Hannah, C.H. Foyer, Low glutathione regulates gene expression and the redox potentials of the nucleus and cytosol in *Arabidopsis thaliana*, Plant Cell Environ. 38 (2015) 266–279.
[78] J. Markovic, N.J. Mora, A.M. Broseta, A. Gimeno, N. de la Concepción, J. Viña, F.V. Pallardó, The depletion of nuclear glutathione impairs cell proliferation in 3t3 fibroblasts, PLoS One 4 (2009) e6413.
[79] P. Díaz-Vivancos, T. Wolff, J. Markovic, F.V. Pallardó, C.H. Foyer, A nuclear glutathione cycle within the cell cycle, Biochem. J. 431 (2010) 169–178.
[80] J. Markovic, José Luís García-Giménez, Amparo Gimeno, José Viña, Federico V. Pallardó, Role of glutathione in cell nucleus, Free Radic. Res. 44 (2010) 721–733.
[81] V. Locato, E. Novo-Uzal, S. Cimini, M.C. Zonno, A. Evidente, A. Micera, C.H. Foyer, L. De Gara, Low concentrations of the toxin ophiobolin A lead to an arrest of the cell cycle and alter the intracellular partitioning of glutathione between the nuclei and cytoplasm, J. Exp. Bot. 66 (2015) 2991–3000.